International Journal of ISSI, Vol.4 (2007), No. 1,2, pp.8-15

Three-dimensional Numerical Simulation of Metal Flow and Solidification in the Multi-cavity Casting Moulds of Automotive Components

A. Kermanpur[1*], Sh. Mahmoudi[2] and A. Hajipour[3]

1- Department of Materials Engineering, Isfahan University of Technology, Isfahan, 84156-83111, Iran
2- Department of Materials and Metallurgical Engineering, Iran University of Science and Engineering, Tehran, Iran
3- Department of Materials Engineering, Isfahan University of Technology, Isfahan,84156-83111, Iran

Abstract

The liquid metal flow and the solidification behaviours in a multi-cavity casting mould of two automotive cast parts were simulated in three dimensions. The commercial code, FLOW-3D® was used because it can track the front of the molten metal by a Volume of Fluid (VOF) method and allows complicated parts to be modeled by the Fractional Area/Volume Obstacle Representation (FAVOR) method. The grey iron automotive components including a brake disc and a flywheel were cast using an automatic sand casting production line. For simulation analysis, the solid models of the casting, the gating system and the ceramic filter were spatially discretised in a multi-block pattern. The surface roughness and the contact angle of the mould were taken into account in the model, based on the properties of the sand mould used. The turbulent flow was simulated using the k-ε turbulence model. The Darcy's law was used to analyse the fluid flow throughout the ceramic filter designed in the gating system. Proper boundary conditions were assigned for the model so that both the simulated filling time and the solidification time were achieved in the range of real experimental measurements. The predicted hot spot of the castings were in agreement with experiments.

The verified simulation model showed that the four-cavity mould used for the flywheel part was more suitable than the three-cavity one of the brake disc, in getting a more uniform fluid flow and heat transfer conditions which causes similar cast parts in each mould. The simulated flow pattern during the mould filling of the castings showed that the first gate of the gating system was not working properly as it remains partially-filled (not pressurised) throughout the half of the filling stage, causing a possible air absorption by the melt. A smaller cross sectional area for the first gate was suggested. The present simulation model is able to analyse different casting parameters of the automatic multi-cavity sand casting process.

Keywords: Numerical simulation, Casting, Solidification, Finite volume method, Automotive components.

Introduction

Numerical simulation provides a powerful means of analysing various physical phenomena occurring during casting processes. It gives an insight into the details of fluid flow, heat transfer and solidification[1,2]. Numerical simulation allows researchers to observe and quantify what is not usually visible or measurable during real casting processes. The goal of such simulations is to help shorten the design process and optimize casting parameters to reduce scrap, use less energy and, of course, make better castings. Simulation produces a tremendous amount of data that characterize the transient flow behaviour (e.g., velocity, temperature), as well as the final quality of the casting (e.g., porosity, grain structure). It takes good understanding of the actual casting process, and experience in numerical simulation, for a designer to be able to relate one to the other and derive useful conclusions from the results.

Accurate representation of the coupled effects between turbulent fluid flow with a free surface, heat transfer, solidification, and mould deformation has been shown to be necessary for the realistic prediction of several defects in castings and also for determining the final crystalline structure [3]. A core component of the computational modeling of casting processes involves mold filling, which is the most computationally intensive aspect of casting simulation at the continuum level. Considering the complex geometries involved in shape casting, the evolution of the free surface, gas entrapment, and the entrainment of oxide layers into the casting make this a very challenging task in every respect. Despite well over 30 years of effort in developing algorithms, this is by no means a closed subject [3].

Most of the casting modelling codes can be divided into two categories: those using the finite difference method (FDM) for solving fluid flow

* *Corresponding author:*
Tel: +98- 311- 3915738 Fax: +98- 311- 3912752
E-mail: ahmad_k@cc.iut.ac.ir
Address: Dept. of Materials Engineering, Isfahan University of Technology, Isfahan, 84156-83111, Iran

1. Assistant Professor
2. M.Sc. Student
3. M.Sc.

equations, and those that employ the finite element method (FEM) [4]. The FE method uses body-fitted computational grids leading to more accurate representation of metal/mould interfaces than generally achievable by FDMs. However, generating good quality FE grids is still a challenging task and often takes significantly more time than the simulation itself. Solution accuracy degenerates in highly distorted grids and changes in geometry, even small ones, often require a completely new grid. The FD method offers ease of mesh generation due to the structured nature of the mesh, uses less storage to describe geometry and simplifies the implementation of the numerical algorithms. However, the conventional FD methods often require fine grids to describe complicated geometry to reduce errors associated with the 'stair-step' representation of curved boundaries. The latter introduces inaccuracies when computing liquid metal flow along the walls and heat fluxes normal to the walls. In order to improve the solution accuracy in modeling mold filling with curved-shape and thin-walled mold cavities, a body-fitted-coordinate (BFC) concept, known as the most effective method to predict a flow field in a curved-shape cavity, has recently been adopted by Hong et al. [5]. In this method, the governing equations for fluid flow are transformed based on the BFC concept.

In this work, the commercial, general purpose, computational fluid dynamics (CFD) code FLOW-3D®, used to simulate the filling and solidification sequences of two automotive components, was cast into a multi-cavity sand mould [6]. The above-mentioned drawbacks are eliminated in this code and will be discussed in the next section.

Model Theory

The CFD code FLOW-3D® is based on the finite volume or finite difference approach. Two methodologies, Fractional Area/Volume Obstacle Representation (FAVOR) and Volume-of-Fluid (VOF), constitute the core of the software. These methods differ from methods in most other codes but offer many advantages, and are summarised below [6].

1) Geometry representation

An advancement of the conventional FD method is given by the FAVOR method. In this method rectangular grid cells can be partially blocked by obstacles [7]. The blockage is described by using fractional cell volumes and areas on cell sides. The FAVOR method improves the accuracy of the numerical solution near mould walls and allows for the use of coarser grids than in standard FD methods. Since the geometry representation is less mesh-dependent, the FAVOR method is also referred to as a 'free gridding' method [4].

For an incompressible and viscous fluid, the FAVOR equations take the form:

$$\nabla \cdot (\mathbf{Au}) = 0 \tag{1}$$

$$\frac{\partial \mathbf{u}}{\partial t} + \frac{1}{V}(\mathbf{Au}\cdot\nabla)\mathbf{u} = -\frac{\mathbf{1}}{\rho}\nabla p + \frac{1}{\rho V}(\nabla \mathbf{A})\cdot(\mu\nabla)\mathbf{u} + g \tag{2}$$

$$\frac{\partial H}{\partial t} + \frac{1}{V}(\mathbf{Au}\cdot\nabla)H = \frac{1}{\rho V}(\nabla \mathbf{A})\cdot(k\nabla T) \tag{3}$$

where,

$$H = \int C(T)\,dT + L(1\text{-}f_s) \tag{4}$$

In these equations A_i is the open area fraction associated with the flow in the ith direction, V the open volume fraction, ρ density, p pressure, u_i the ith velocity component, μ the fluid viscosity coefficient, g gravity, H fluid enthalpy, T fluid temperature, f_s solid fraction, L latent heat, and C and k fluid specific heat and thermal conductivity coefficient, respectively. All bold parameters are vector. For the mould, the energy equation has the form

$$\frac{\partial T_m}{\partial t} = \frac{1}{\rho_m C_m V_c}\left(\nabla \mathbf{A_c}\right)\cdot\left(k_m \nabla T_m\right) \tag{5}$$

where the subscript m indicates a parameter related to the mould and the subscript c indicates quantities that are complements of the volume and area fractions. At the metal/mould interface, the heat flux, q, is calculated according to

$$q = h(T - T_m) \tag{6}$$

where h is the heat transfer coefficient.

2) Tracking the free surface

Mould filling problems involve tracking free surfaces that are the boundaries between liquid metal and the surrounding air. The most commonly used method to describe free surfaces is the Volume-of-Fluid (VOF) method. The VOF method enables the tracking the transient free surfaces with arbitrary topology and deformations (e.g., fluid surface break-up and coalescence). The 'true' VOF method consists of three main components [8]:

1. A fluid volume fraction function $F(t,r)$ which is equal to 1.0 in fluid regions, to 0.0 in voids (on air) and between 0.0 and 1.0 for free surface. Since fluid configurations may change with time, F is a function of time, t, as well as space, $\boldsymbol{r}$. Averaged over a computational control volume, the fluid fraction function has a fractional value in cells containing a free surface.
2. Zero shear stress and constant pressure boundary conditions are applied at free surfaces.
3. A special advection algorithm is used for tracking sharp free surfaces.

The equation for the F function is

$$\frac{\partial F}{\partial t} + \frac{1}{V}\nabla \cdot (\mathbf{A}uF) = 0 \tag{7}$$

The boundary conditions at the free surface are zero normal and tangential stresses.

A free-surface advection method must preserve the sharpness of the interface and have minimal free

surface distortion. Generally, such advection algorithms are based on geometric reconstruction of the free surface using the values of F at grid nodes [9]. Sometimes a free surface is approximated by a density discontinuity between metal and air and flow equations are solved for both fluids. In that case it is difficult to enforce correct boundary conditions at the surface. This is because free surface pressure and velocities in the two-fluid approach are not set explicitly, but are computed by solving the flow equations and these flow equations are solved in terms of mixture variables. Since densities of liquid metal and air differ greatly (*e.g.*, by a factor of 6,000 for steel), the mixture velocity may not always be an accurate measure of the relative motion of metal and air [9].

Numerical Simulation

Two automotive components including a brake disc and a flywheel were simulated in this work. The complete solid models of the parts were created in steriolithography (STL) format and imported to the software (Figure 1).

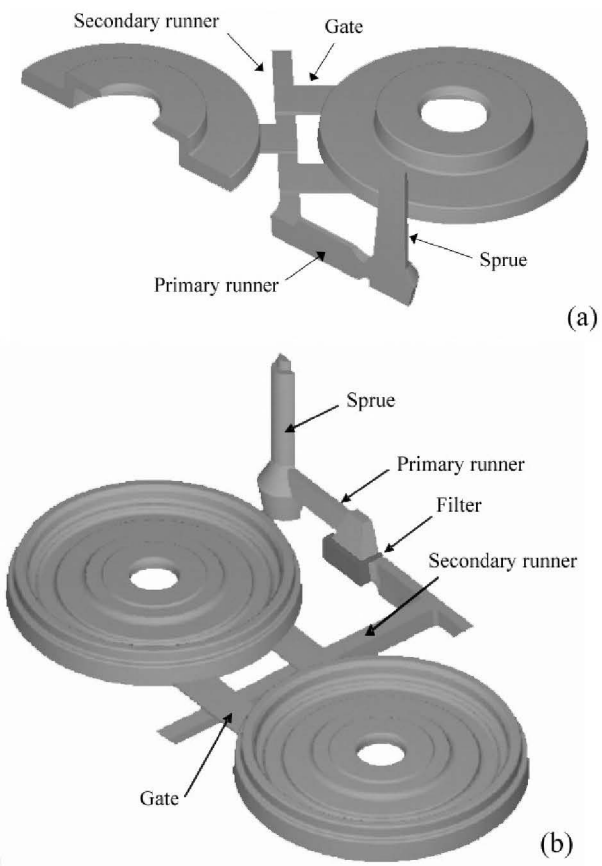

Fig. 1. The solid models of the automotive components:
(a) three-cavity brake disc and (b) four-cavity flywheel. Note that due to the symmetry, only half of the whole mould is modelled.

Due to the symmetry plane of the system, only half of each model was modelled. Different meshes were tested for both castings, among them the multi-block meshes were found more efficient and less expensive. The multi-block meshes of the models are shown in Figure 2.

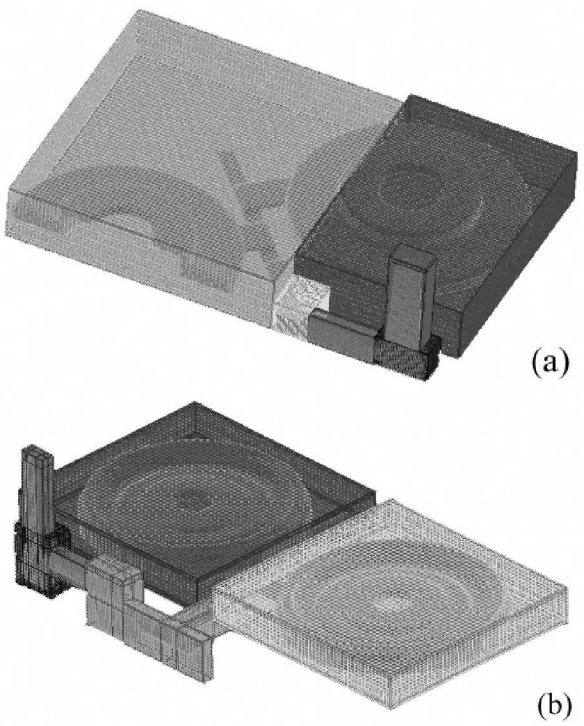

Fig. 2. The multi-block meshes of the castings:
(a) brake disc and (b) flywheel. Note that the mould mesh is not shown.

The mesh size for the cast parts and different blocks of the gating system were 4 and 1.5mm, respectively. The melt was gray cast iron whose chemical composition is listed in Table 1. Thermo-physical properties of the cast iron parts, silica mould and ceramic filter, were derived from both literature and manufacturer's documents and are listed in Table 2. The initial and boundary conditions of the system are shown in Table 3. Depth of surface roughness of the mould is approximately that of the dimensions of the sand grains [10]. The pouring velocity of the melt entering the sprue was assigned based on the calculation of the total weight of the melt and the experimentally- measured filling time. The heat transfer coefficient between the mould wall and the casting was computed from the measurement of the total solidification time for each casting [11]. The following assumptions were considered in the simulations [6]:

1. Incompressible, Newtonian flow.
2. k-ε Turbulence model.
3. Darcy's model for the porous media.

Table 1. Chemical composition of the cast iron (wt%)

Element	C	Si	Mn	Sn	Cr	S	P	Fe
Wt%	3.38	0.1	0.71	0.02	0.05	0.01	0.01	rem

Table 2. Thermo-physical properties of the casting, mould and filter

Material	Property	Symbol	Value	Unit
Casting	Thermal conductivity of liquid	k_l	39.59	W/m/K
	Thermal conductivity of solid	k_s	34.39	W/m/K
	Specific heat of liquid	C_l	897	J/kg/K
	Specific heat of solid	C_s	770	J/kg/K
	Surface tension coefficient of liquid	σ	1.871	kg/s^2
	Kinematic viscosity	μ	0.0045	m^2/s
	Density of liquid	ρ_l	6856	kg/m^3
	Density of solid	ρ_s	7100	kg/m^3
	Latent heat	L	216	kJ/m^3
	Liquidus temperature	T_l	1504	K
	Solidus temperature	T_s	1420	K
Silica sand mould	Thermal conductivity	k_m	0.61	W/m/K
	Volumetric specific heat	$\rho_* C$	1700	kJ/kg/K
Alumina ceramic filter	Thermal conductivity	k_f	1.6	W/m/K
	Volumetric specific heat	$\rho_* C$	4660	kJ/kg/K
	Porosity		0.4	---

Table 3. Initial and boundary conditions of the system

Condition	Value	Unit
Initial temperature of melt	1703	K
Initial temperature of mould	293	K
Pouring velocity of melt	3.0 (for barke disc) 4.5 (for flywheel)	m/s
Heat transfer coefficient between casting and mould	600	W/m^2K
Surface roughness of mould surface	25×10^{-6}	m
Contact angle of mould surface	180	deg.

Within a porous body, the flow of a fluid is resisted by viscous and geometric (tortuosity) effects [6]. Flow losses in porous media can be modelled in a number of ways. Most common case is the Darcy type flow in which the flow resistance is linearly proportional to velocity. Saturated flow in porous media is one such application. Another case might be the flow of air through a matrix of fibers as in a filter apparatus. For these cases, FLOW-3D® software has provisions for a volume fraction (or porosity) dependent drag coefficient, K,

$$K = aV_F^{-b} \tag{8}$$

where a and b are positive constants and V_F is the fractional volume open to flow. A zero value of b can be used when a constant drag coefficient is desired. The constants of the drag coefficient equation were assigned based on the data delivered by the filter manufacturer. Flow in porous media and the solidification/melting model use a drag force proportional to the first power of the velocity, $-Ku$. These models assume the possibility of an arbitrarily large drag coefficient, K, in which the momentum equations may reduce to a balance between drag and pressure gradient forces. To compute in this high drag limit for incompressible flow, it is necessary to treat the drag terms implicitly, not only in the momentum equations but also in the continuity equation. This is accomplished by using the time-advanced value for the velocity in the drag term and algebraically solving the difference equation for the new velocity. The result is a division of all contributions to the new velocity by the term $(1+K\delta t)$. Keeping the effect of this extra term throughout all pressure/velocity adjustments then ensures that a balance between pressure gradient and drag forces can be achieved that also satisfies the continuity equation.

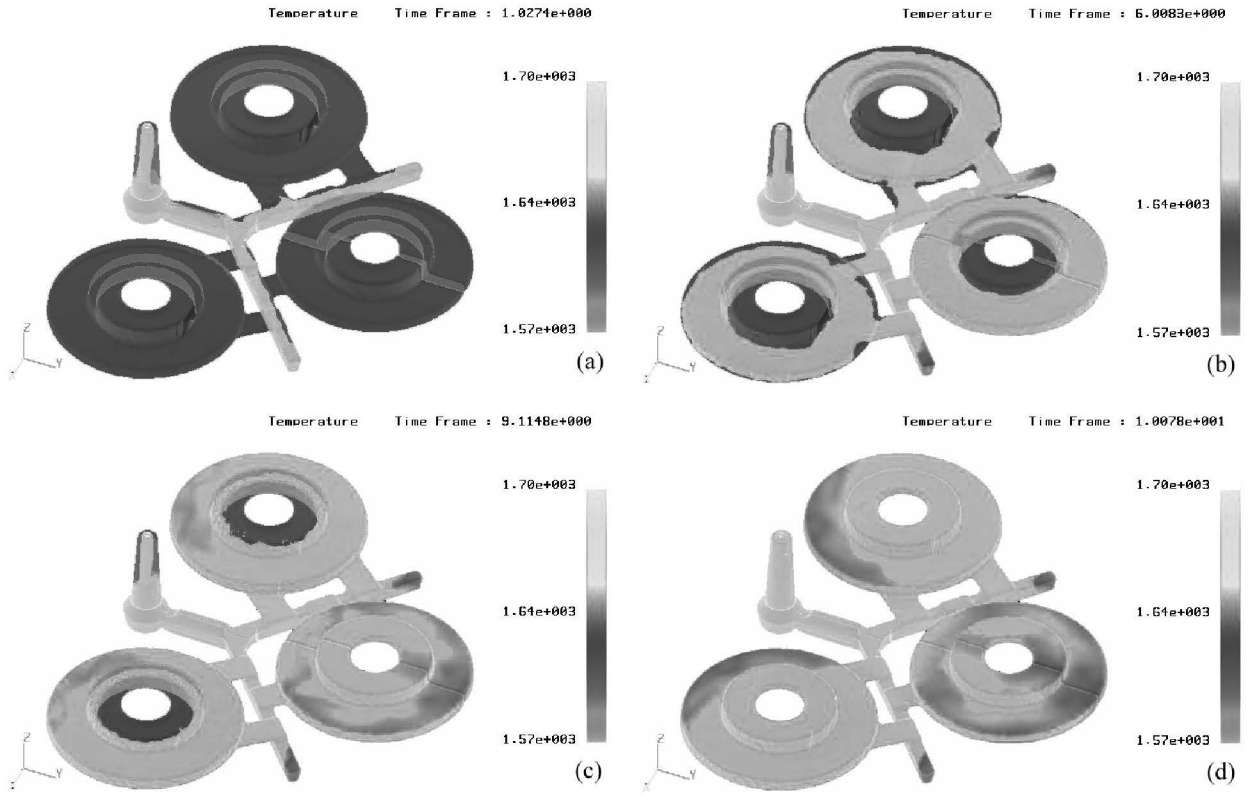

Fig. 3. The filling sequences for the brake disc part cast in a three-cavity sand mould at different lengths of time: (a) 1.0 s, (b) 6.0 s, (c) 9.1 s, and (d) 10.1 s.

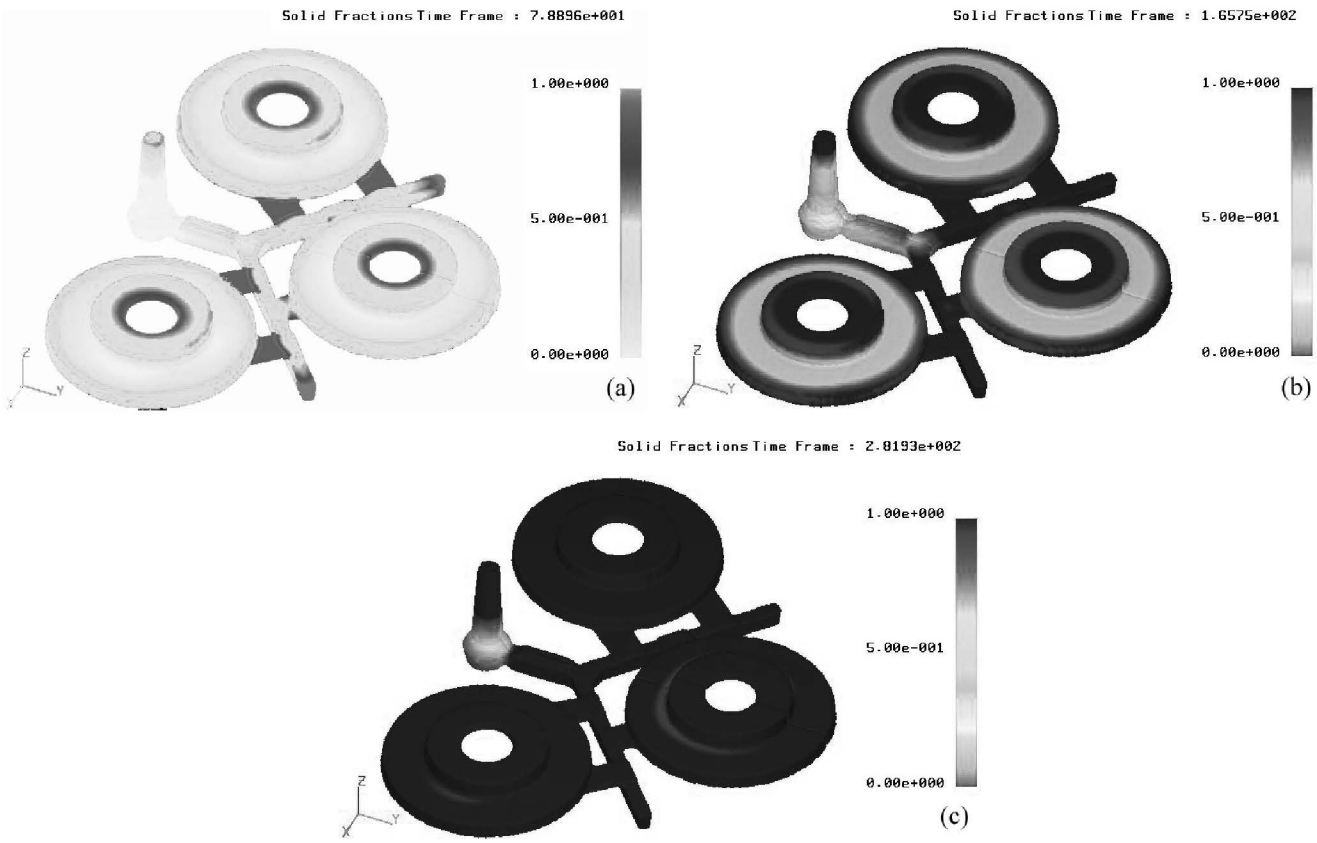

Fig. 4. The solidification sequences for the brake disc part cast in a three-cavity sand mould at different lengths of time: (a) 78.9 s, (b) 165.8 s, and (c) 281.9 s.

Results

1) Brake disc part

The filling pattern of the three-cavity brake disc mould is shown in Figure 3. The cast iron melt stream with a cross sectional area less than that of the sprue is entered into the mould and fills up the primary runner followed by the secondary runner after about 1.0 s (Figure 3a). The melt is then entered to the mould cavity through the second gate of the side-castings followed by the gates of the middle-casting, when the inclusion trap in the primary runner is completely filled. During the filling of the mould, it can be seen that the first gates of the side-castings are remained partially-filled (not pressurised) even until about 6.0 s during which the melt might suck the air through the mould (Figure 3b). The mould filling process proceeds such that the middle-cavity is completely filled up sooner than the side-cavities (Figures 3c & 3d).

The solidification pattern of the brake disc component just after filling is shown in Figure 4. The melt solidification is started around the gates such that all gates are completely solidified after about 80 s (Figure 4a). The solidification follows from the low modulus sections like the internal and external edges towards the casting centre. The secondary runner is completely solidified after about 166 s (Figure 4b). The side-castings and the middle-casting are finally solidified after 280 s and 300 s, respectively (Figure 4c).

2) Flywheel part

The filling pattern of the four-cavity flywheel mould is shown in Figure 5. The cast iron melt stream with a cross sectional area less than that of the sprue is entered into the mould and after passing the filter, fills up the primary runner at about 0.5 s (Figure 5a). Note that the porous-media filter is shown as a transparent region. The secondary runner is then filled up, raising the melt level in the sprue. It is after about 1.1 s that the melt enters the gates and starts filling the cavities slowly (Figure 5b). The simulated flow pattern shows that the first gate of all four castings in the mould remains *partially-filled* even until about 6.9 s (Figure 5c). The rest of the mould cavity is then filled up smoothly. As it is shown in Figure 5, the predicted filling time is about 15.5 s that is in agreement with the observations (Figure 5d). It is also seen that two cavities closer to the sprue are filled up sooner (about 0.2 s) than the others.

The solidification pattern of the flywheel cast parts just after filling is shown in Figure 6. The melt solidification is started around the filter, top of the sprue and end of the secondary runner followed by the gates (Figure 6a). After about 100 s, all gates as well as the filter chamber are completely solidified and the solidification of the cast part starts from the edges (Figure 6b). The solidification of all castings

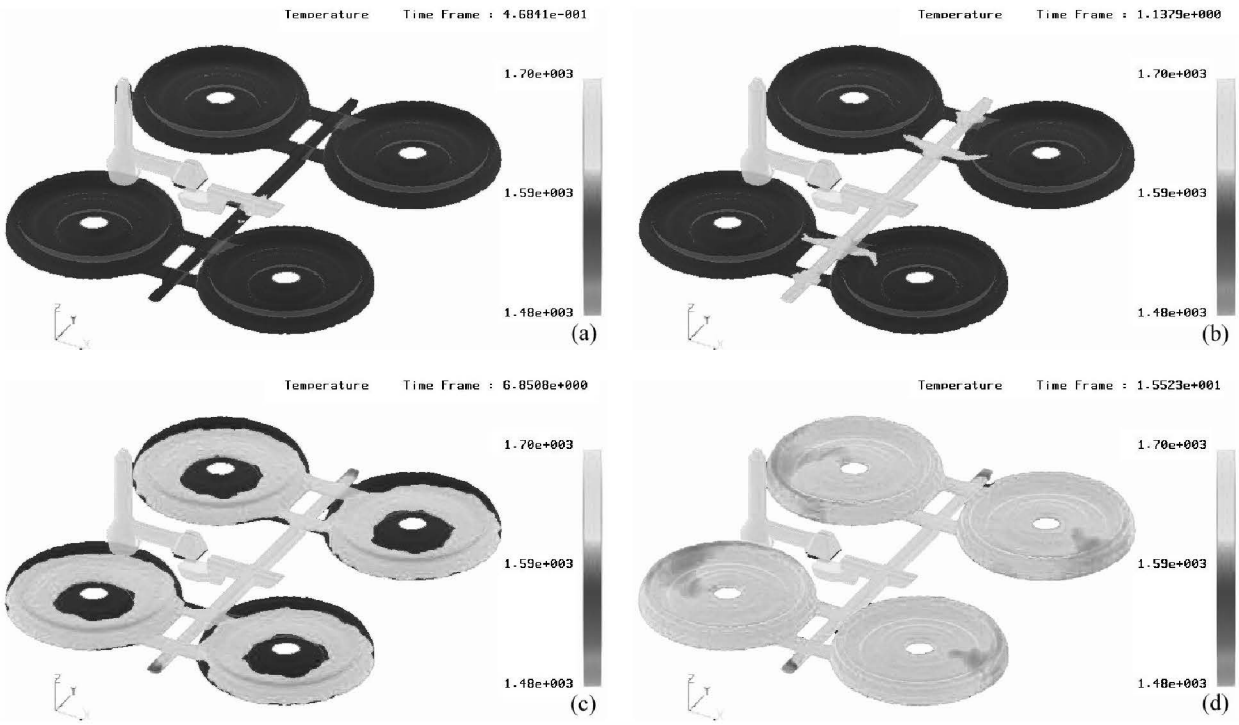

Fig. 5. The filling sequences for the flywheel part cast in a four-cavity sand mould at different lengths of time: 0.47 s, (b) 1.14 s, (c) 6.85 s, and (d) 15.52 s. Note that the filter is not shown in the figures.

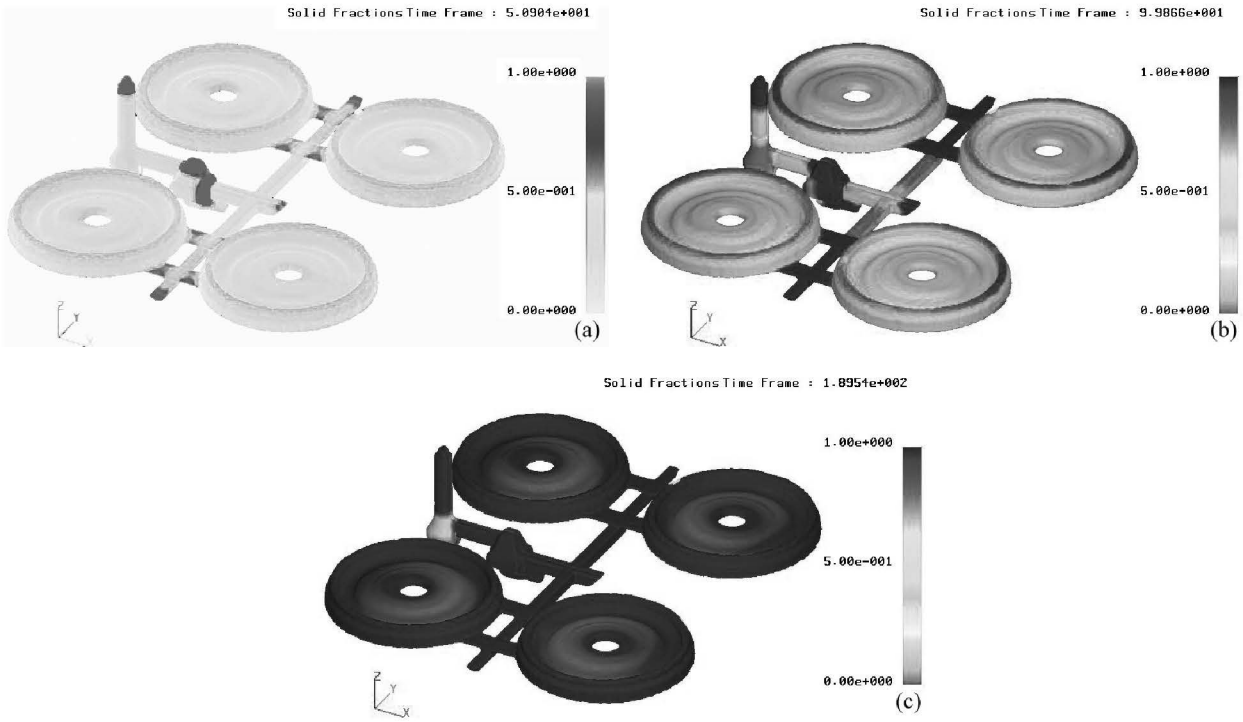

Fig. 6. The solidification sequences for the flywheel part cast in a four-cavity sand mould at different lengths of time: (a) 50 s, (b) 100 s, and (c) 190 s.

takes place simultaneously about 220 s and the rest of the gating system solidifies approximately 50 s afterwards (Figure 6c). This uniform solidification pattern shows a relatively suitable gating system design which can lead to a reasonable casting efficiency.

Discussion

As mentioned in the "Numerical Simulation" section above, the flow and thermal boundary conditions of the simulation model were both assigned based on the experimental validation of the filling and solidification times of the cast parts. The verified model interestingly represented the correct location of the hot spots in the castings. Figure 7 compares the simulated result of the final location of the hot spots for the brake disc with the micro-shrinkage that is experimentally observed for some castings, showing a reasonable agreement. It should be noted that became the automatic moulding system was being used, it was not possible to propose a suitable chilling system to fully avoid such micro-shrinkage. However, the simulation results showed that decreasing the superheat temperature is a practical parameter to significantly reduce the occurrence of such possible micro-shrinkage at this location [12].

The simulated results for liquid metal flow pattern during casting of both cast parts (see Figures 3b & 5c) showed that the first gate of the gating system has not been designed work properly, as it remains *partially-filled* until about half of the mould filling period. This manner can cause air absorption by the melt, resulting in possible gas porosity in the final parts. It is suggested that in order to make the first gate full, its cross sectional area should be reduced. This will not affect the flow pattern in the system. Another suggestion is to use a stepped-gate instead of using the gate with a uniform cross sectional area. This suggestion was tested successfully in the previous work [13].

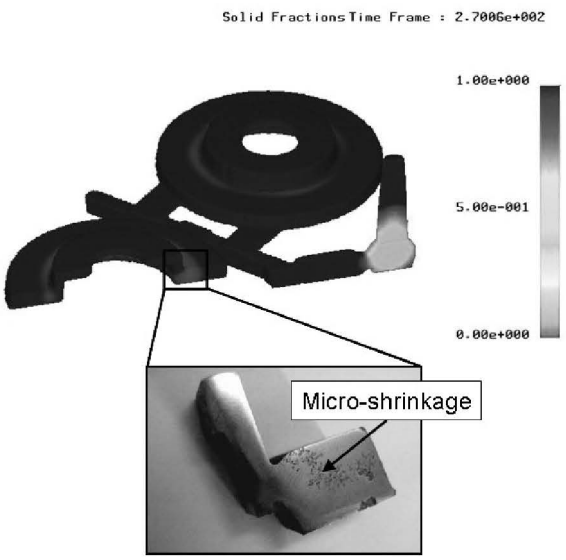

Fig. 7. Comparison of predicted result for the hot spot with a micrograph of the cross section of the brake disc. The figure shows a good agreement between simulation and experiment.

Comparison between the flow pattern of the flywheel and the brake disc shows that using filter in the gating system can also reduce turbulence of the melt, regardless of removing the inclusions. This can be a benefit for lowering probability of melt oxidation or sand erosion as well.

The simulation results for both castings clearly demonstrate that all gates are properly solidified prior to the castings, making it possible for the melt to compensate its contraction during solidification by the expansion of graphite phase such that no riser is needed. Therefore, in terms of the solidification point of view, the cross sectional area of the gates are designed satisfactory.

The solidification behaviour of the three-cavity brake disc mould showed a non-uniform manner for the side-castings compared to the middle-casting. On the other hand, the four-cavity flywheel mould represented uniform solidification behaviour for all cast parts. It can be concluded that in order to establish similar heat transfer and solidification conditions for all cast parts in each multi-cavity mould, it is better to consider symmetrical configuration. Therefore, a four-cavity mould is suggested for the brake disc part.

The present simulation model clearly shows the capability of evaluating the fluid flow and solidification behaviours of the automatic sand casting process. This model is even capable of investigating the casting efficiency as well as testing the suitability of different gating system designs. The model is under development for tracking inclusion during the mould filling.

Conclusions

A 3D simulation model was developed to simulate the filling and solidification behaviours of the automotive components, cast in an automatic sand casting production line. The verified model based on the experimental observations showed that the four-cavity mould is more suitable than the three-cavity one in getting a more uniform casting quality for all cast parts. The model also represented a different performance between the gates for each cast part, suggesting a smaller cross sectional area for the first gate to reduce the risk of air absorption. The present simulation model is able to study the effects of several casting parameters including the melt superheat, pouring time (velocity), mould surface roughness, gating design, and the mould configuration on the quality and soundness of automotive cast parts.

Acknowledgment

The authors appreciate the collaboration of their colleagues at Isfahan University of Technology and Azarin Casting Industries of Isfahan, especially Mr. H. Morady.

References

[1] M. C. Flemings, Solidification Processing, McGraw-Hill Book Co., New York, (1974), 10.
[2] J. Campbell, Castings, Butterworth Heinmann, (1991), 31.
[3] M. Cross, K. Pericleous, T. N. Croft, D. McBride, J. A. Lawrence and A. J. Williams: Metall. Mater. Trans. B, 37(2006), 879.
[4] M. R. Barkhudarov, Advanced simulation of the flow and heat transfer in simultaneous engineering, Technical Report, Flow Science, Inc , (1998).
[5] C. P. Hong, S. Y. Lee, and K. Song, ISIJ International, 41(2001), 999.
[6] FLOW-3D® User's Manual, Flow Science, Inc., Version 8.2, (2005).
[7] M. R. Barkhudarov and C. W. Hirt, Casting simulation: mold filling and solidification–benchmark calculations using FLOW-3D®, Technical Report, Flow Science, Inc , (1993).
[8] C. W. Hirt and J.M. Sicilian, Proc. of the 4th International Conference on 'Ship Hydrodynamics', Washington, DC, (1985), 450.
[9] C. W. Hirt and B. D. Nichols, J. Computational Physics, 39 (1981), 201.
[10] Metals Handbook, Volume 15, Casting, ASM International, (1988), 545.
[11] D. B. Kothe and W. J. Rider, Comments on modelling interfacial flows with Volume-of-Fluid methods, Los Alamos National Laboratory Report LA-UR-94-3384, (1994).
[12] A. Kermanpur, Sh. Mahmoudi and A. Hajipour, Proc. of the 8th Symposium of the Iron and Steel Society of Iran, Isfahan University of Technology, (2006), 188.
[13] A. Kermanpur, A. Hajipour, and Sh. Mahmoudi, Proc. of the 14th Annual (International) Mechanical Engineering Conference (ISME2006), Isfahan University of Technology, Isfahan, (2006), 104.